



STRUCTURAL SCIENCE
CRYSTAL ENGINEERING
MATERIALS

Volume 76 (2020)

Supporting information for article:

Crystal structures of two furazidin polymorphs revealed by a joint effort of crystal structure prediction and NMR crystallography

Marta K. Dudek, Piotr Paluch and Edyta Pindelska

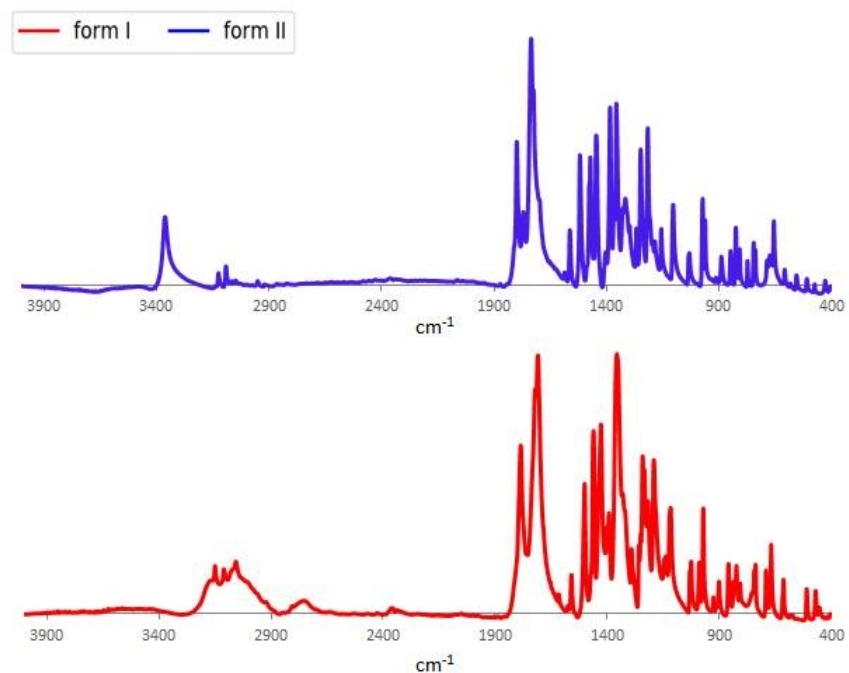


Figure S1. FT-IR spectra of furazidin form I and II.

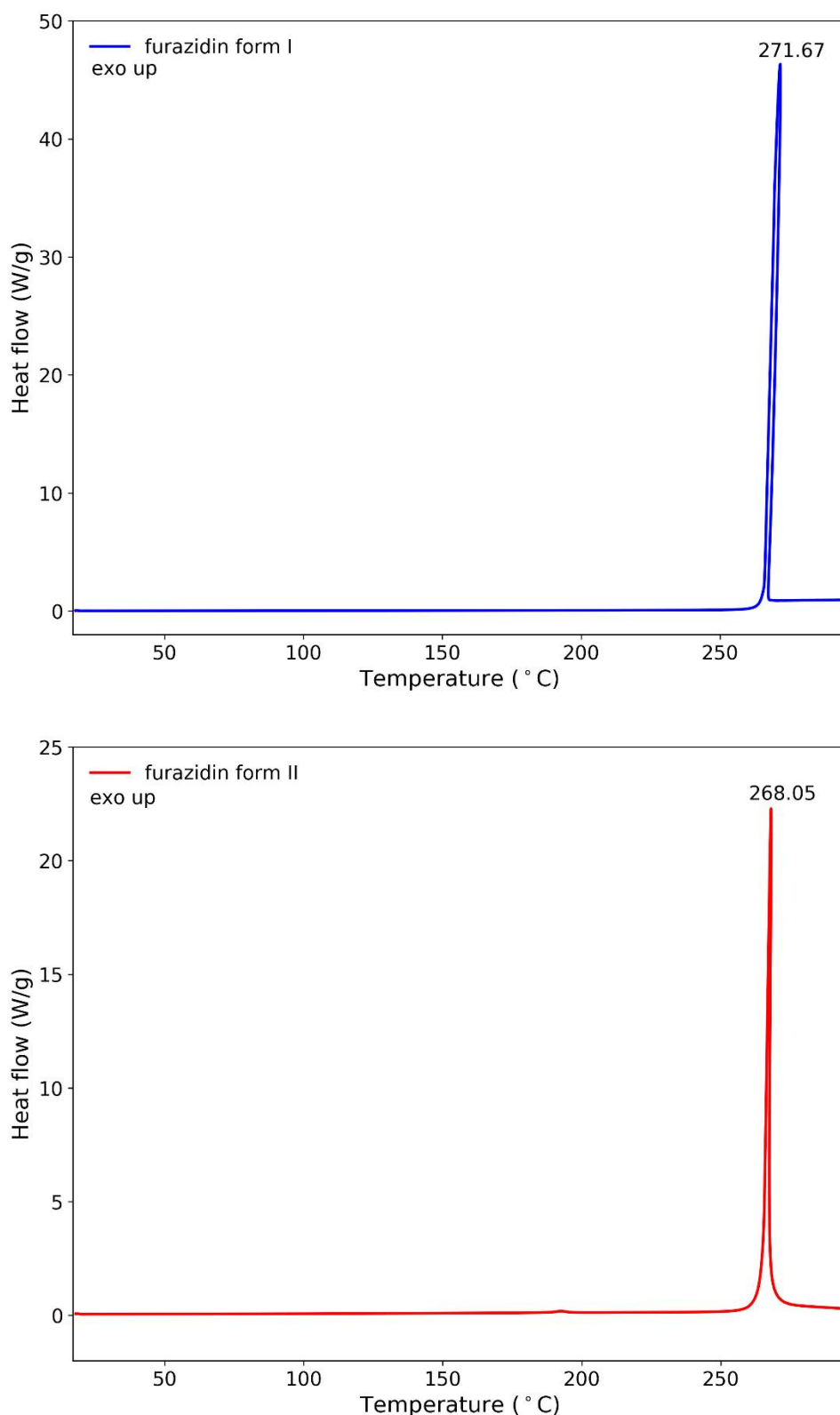


Figure S2. DSC for furazidin form I and II at scan rate 2 K/min. The shown temperatures correspond to the melting/decomposition points, while the respective enthalpies of fusion for the observed exothermic events are equal to 1231 and 1205 J/g. Note, however, that due to a significant amount of

heat emitted during these events the given values may be burdened with error. A small exothermic event at 192 °C is associated with a weight loss of 0.23% of the sample of furazidin form II (see TGA plot below, registered in the temperature range of 20 – 220 °C) and is not reversible, nor visible in the second run of heating, therefore it is probably associated with a decomposition of a small amount of impurities present in the sample. The performed experiments indicate that forms I and II are enantiotropic polymorphs.

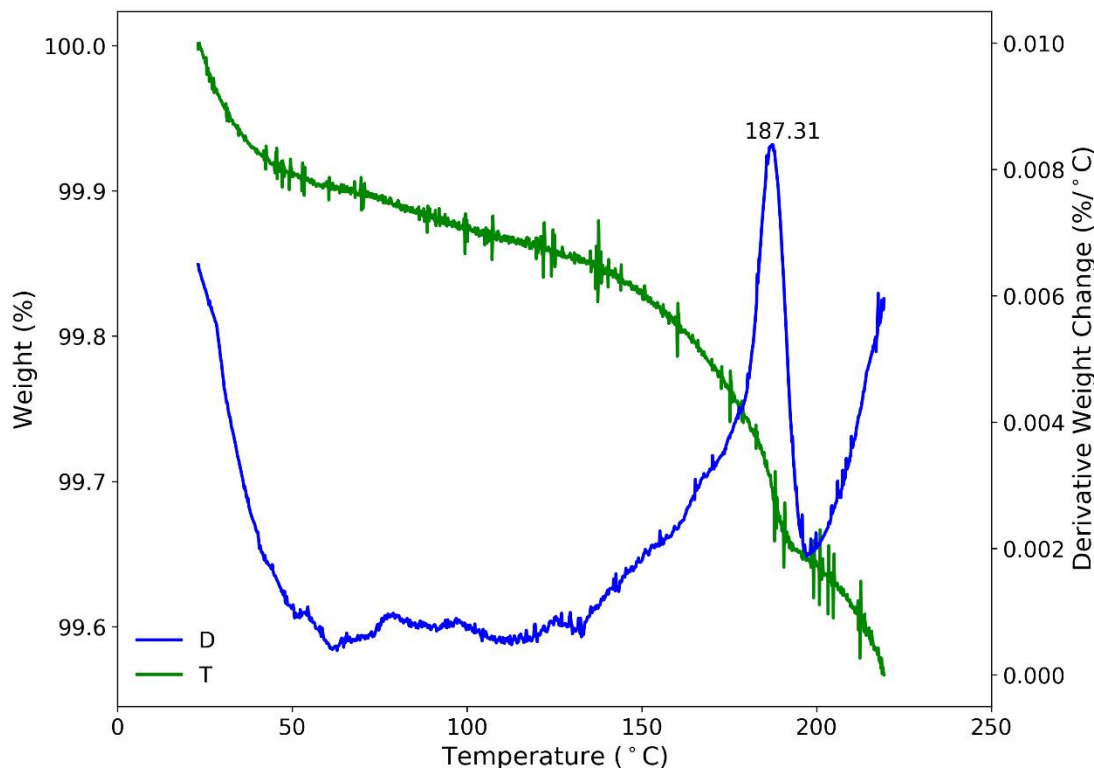


Figure S3. TGA and DTA plots registered for furazidin form II in the temperature range of 20 – 220 °C showing 0.23% weight loss associated with an exothermic event observed in the DSC plot at 192 °C.

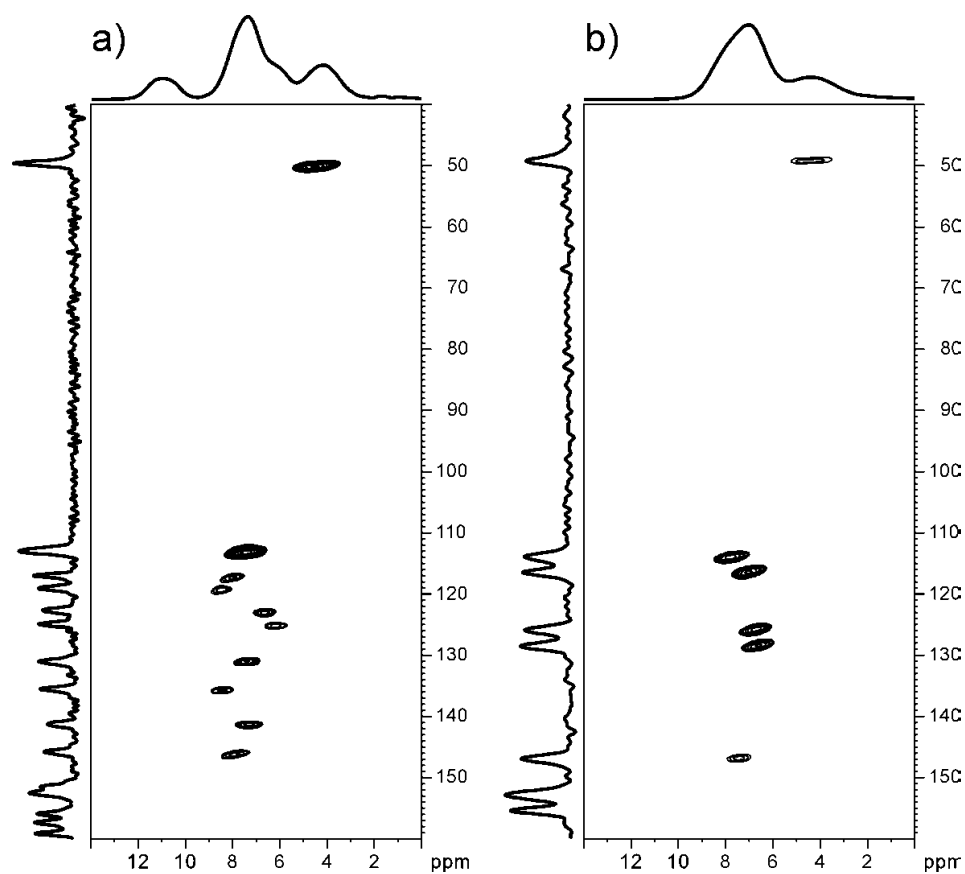
Additional solid-state NMR spectra registered for form I and II of furazidin

Figure S4. inv^{-1}H - ^{13}C HETCOR spectrum registered with short second contact time ($50 \mu\text{s}$) for furazidin form I (a) and (II); spinning speed = 60 kHz ; spectrum a) was registered at an 800 MHz spectrometer to obtain good separation of correlation peaks, whereas spectrum b) was registered with a 600 MHz spectrometer.

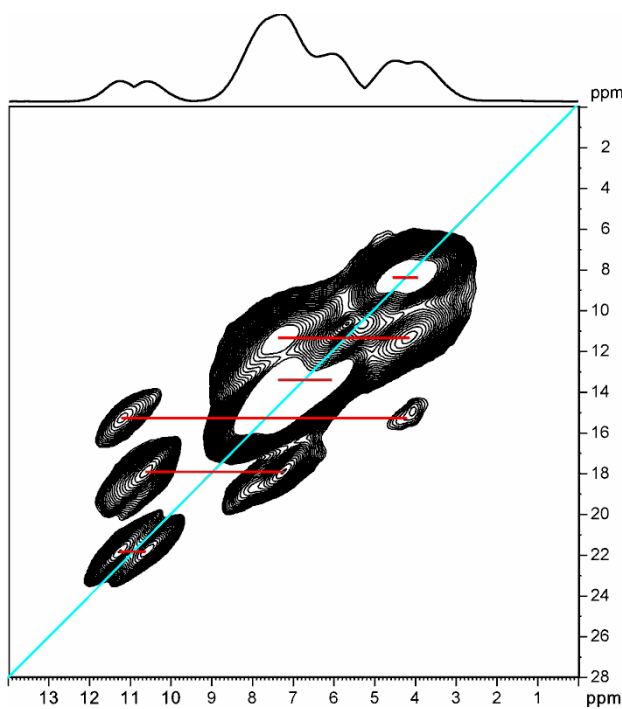


Figure S5. ^1H - ^1H Back-to-Back correlation spectrum for furazidin form I; spinning speed = 60 kHz.

Additional CSP crystal energy landscapes for $Z' = 2$ structure of furazidin

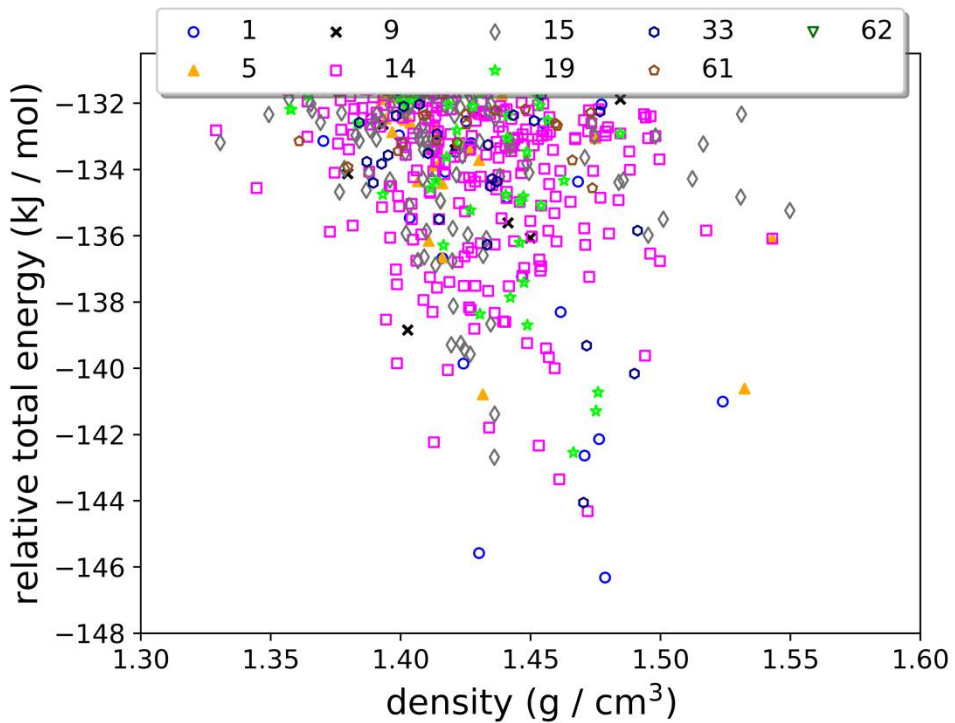


Figure S6. Crystal energy landscape obtained after CSP search for the pair of conformer indicated by comparison with NMR experiments in space groups P1, C2, Cc, P2₁/c, C2/c, P2₁2₁2₁, Pna2₁, Pbca and Pnma

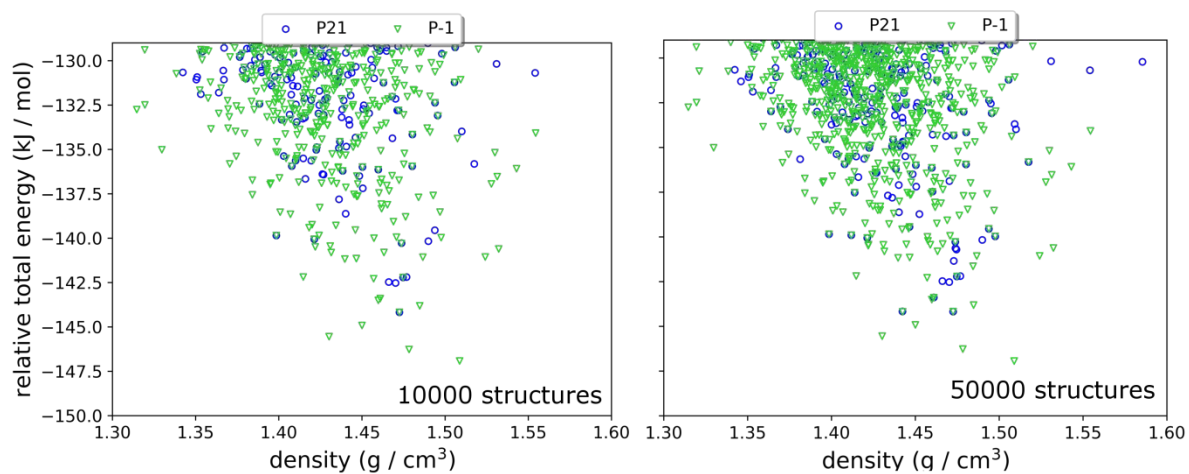


Figure S7. Comparison of CSP landscapes for the selected pair of conformers tested in P2₁ and P-1 space groups, in which 10000 or 50000 valid crystal structures were generated.

The assignment of ^1H and ^{13}C solid-state NMR chemical shifts for forms I and II of furazidin

Table S1. ^1H and ^{13}C solid-state NMR chemical shifts of furazidin form II

atom	$\delta(^{13}\text{C})$	$\delta(^1\text{H})$
C2	155.4	
C3	113.9	7.8
C4	116.3	7.0
C5	152.8	
C α	125.7	6.75
C β	128.4	6.6
C γ	146.9	7.4
C2'	152.8	
C4'	167.2	
C5'	48.8	4.7; 4.0
NH		8.1

Table S2. Two variants of the assignment of ^1H and ^{13}C solid-state NMR chemical shifts of furazidin form I

molecule	atom	variant I		variant II	
		$\delta(^{13}\text{C})$	$\delta(^1\text{H})$	$\delta(^{13}\text{C})$	$\delta(^1\text{H})$
A	C2	157.4		159.2	
	C3	113.1	7.2	113.1	7.0
	C4	119.1	7.8	119.1	7.8
	C5	151.8		151.8	
	C α	125.0	5.8	122.8	6.4
	C β	131.2	7.3	135.5	8.2
	C γ	141.3	6.95	141.3	6.95
	C2'	152.8		152.8	
	C4'	173.6		173.6	
	C5'	49.6	4.5; 4.2	49.6	4.5; 4.2
NH		10.8		10.8	

B	C2	159.2		157.4
	C3	113.1	7.0	113.1
	C4	117.1	7.6	117.1
	C5	151.8		151.8
	Calpha	122.8	6.4	125.0
	Cbeta	135.5	8.2	131.2
	Cgamma	145.9	7.3	145.9
	C2'	155.9		155.9
	C4'	167.3		167.3
	C5'	49.6	4.1; 3.9	49.6
	NH		11.3	11.3

Comparison of simulated and experimental PXRD diffractograms for form I and II of furazidin

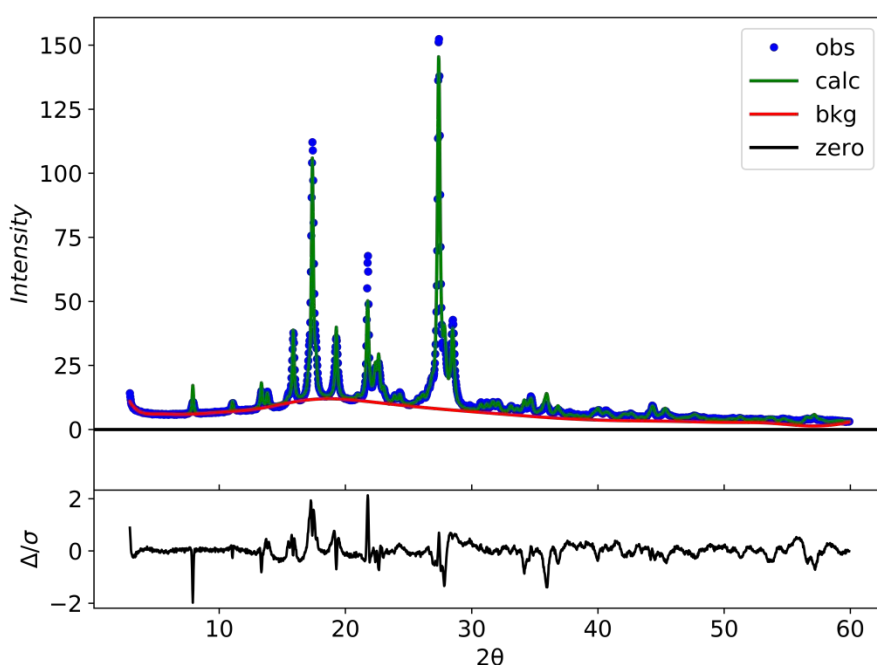


Figure S8. Overlay of the experimental and simulated PXRD diffractogram for furazidin form II.

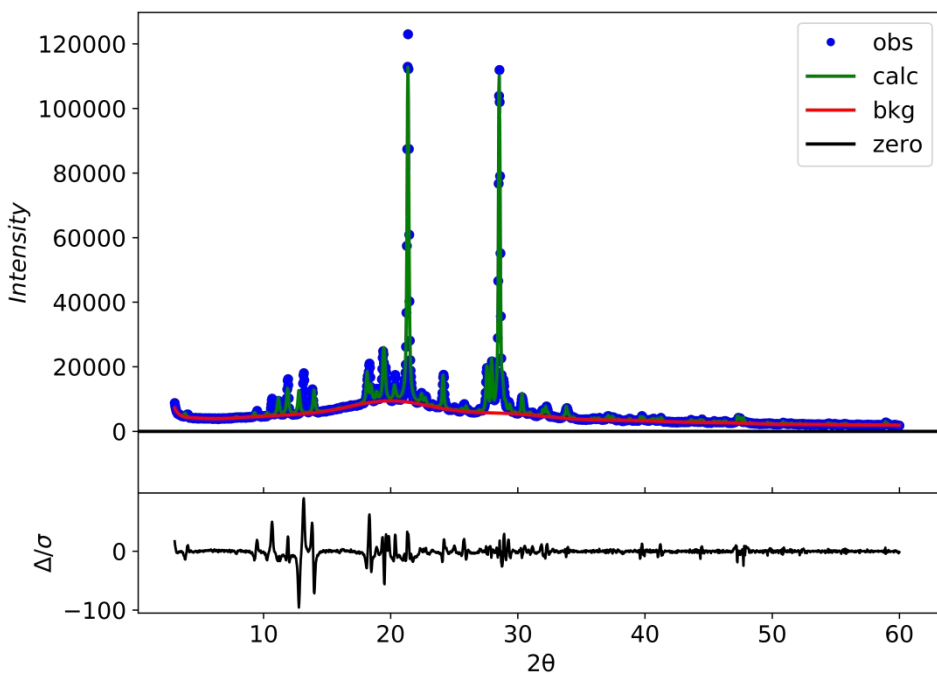


Figure S9. Overlay of the experimental and simulated PXRD diffractogram for furazidin form I.

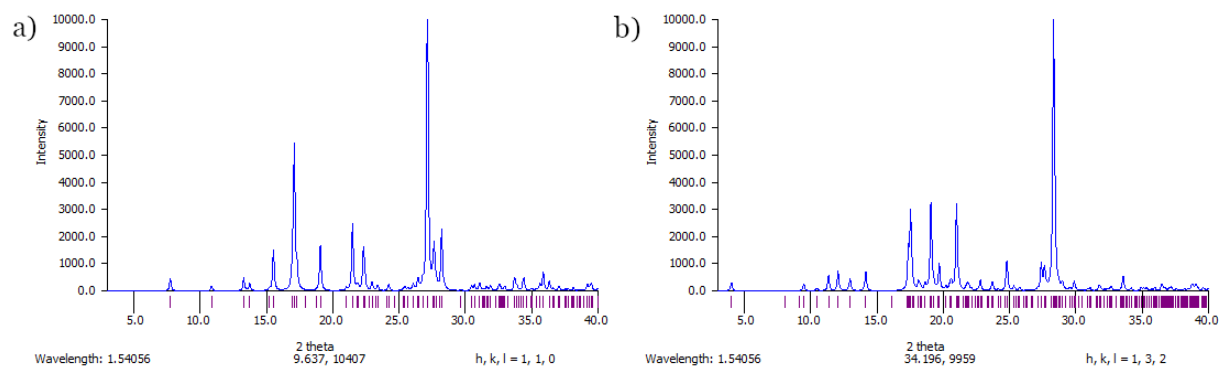


Figure S10. Simulated PXRD patterns for computationally generated structures of form II (a) and I (b).

Hirshfeld surfaces and energy frameworks for calculated for crystal structures of form I and II of furazidin

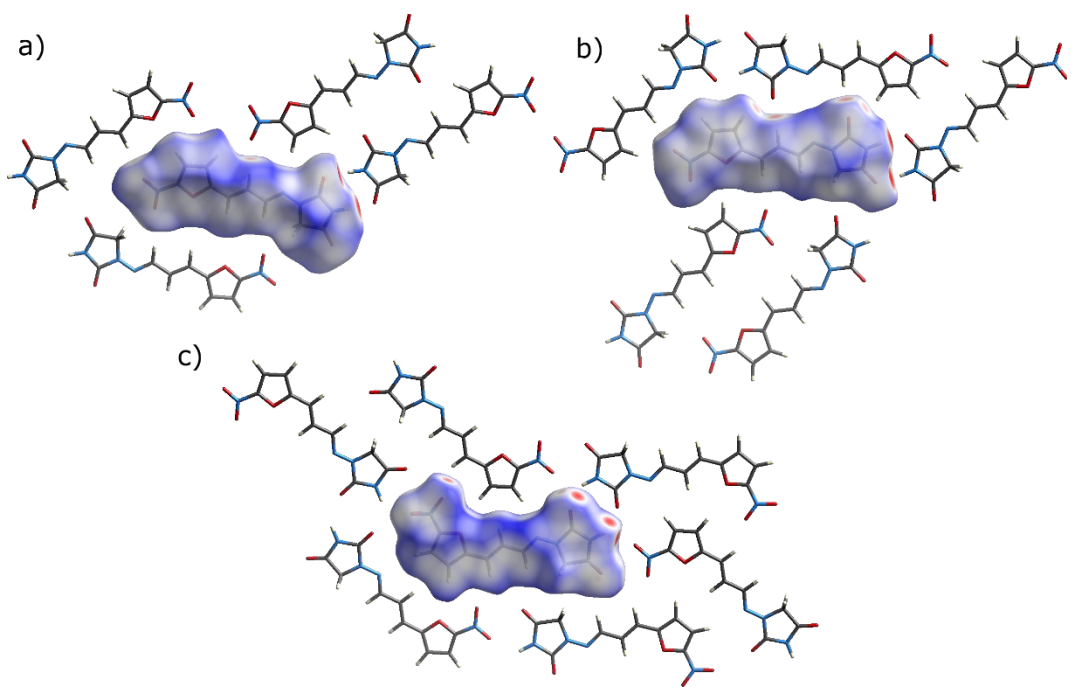


Figure S11. The HSs mapped with d_{norm} for furazidin molecules: a) form I, molecule A, b) form I, molecule B, and c) form II

Table S3. The interaction energies (kJ/mol) obtained from energy framework calculation for furazidin form I molecule A.

	N	Symop	R	Electron Density	E_ele	E_pol	E_dis	E_rep	E_tot
	0	x, y, z	5.33	B3LYP/6-31G(d,p)	-4.9	-5.4	-33.2	18.1	-26.9
	0	-x, -y, -z	7.36	B3LYP/6-31G(d,p)	-25.7	-9.5	-18.2	35.7	-27.9
	0	-x, -y, -z	7.74	B3LYP/6-31G(d,p)	-17.4	-3.7	-30.3	12.6	-39.8
	1	-	9.81	B3LYP/6-31G(d,p)	-2.6	-0.1	-0.6	0.0	-3.4
	1	-	13.67	B3LYP/6-31G(d,p)	-4.9	-5.4	-33.2	18.1	-26.9
	1	-	7.58	B3LYP/6-31G(d,p)	-25.7	-9.5	-18.2	35.7	-27.9
	0	-x, -y, -z	12.54	B3LYP/6-31G(d,p)	-12.1	-2.2	-11.4	5.9	-20.7
	0	-x, -y, -z	15.75	B3LYP/6-31G(d,p)	4.1	-0.2	-1.0	0.1	3.4
	2	x, y, z	5.33	B3LYP/6-31G(d,p)	-4.9	-5.4	-33.2	18.1	-26.9

Table S4. The interaction energies (kJ/mol) obtained from energy framework calculation for furazidin form I molecule B.

	N	Symop	R	Electron Density	E_ele	E_pol	E_dis	E_rep	E_tot
	2	x, y, z	5.33	B3LYP/6-31G(d,p)	-4.9	-5.4	-33.2	18.1	-26.9
	1	-x, -y, -z	7.36	B3LYP/6-31G(d,p)	-25.7	-9.5	-18.2	35.7	-27.9
	1	-x, -y, -z	7.74	B3LYP/6-31G(d,p)	-17.4	-3.7	-30.3	12.6	-39.8
	1	-	9.81	B3LYP/6-31G(d,p)	-2.6	-0.1	-0.6	0.0	-3.4
	1	-	13.67	B3LYP/6-31G(d,p)	-4.9	-5.4	-33.2	18.1	-26.9
	1	-	7.58	B3LYP/6-31G(d,p)	-25.7	-9.5	-18.2	35.7	-27.9
	1	-x, -y, -z	12.54	B3LYP/6-31G(d,p)	-12.1	-2.2	-11.4	5.9	-20.7
	1	-x, -y, -z	15.75	B3LYP/6-31G(d,p)	4.1	-0.2	-1.0	0.1	3.4

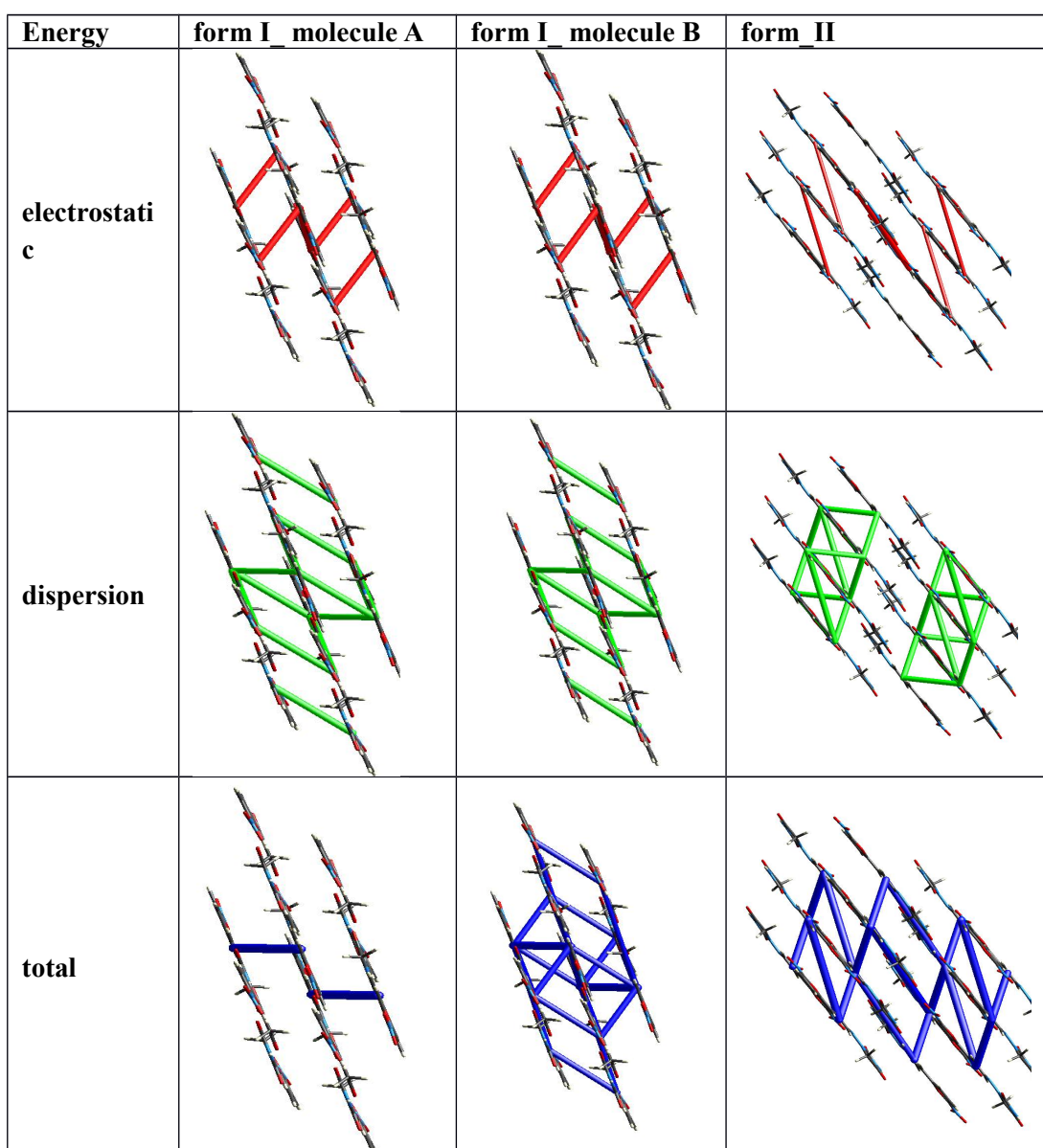
Table S5. The interaction energies (kJ/mol) obtained from energy framework calculation for furazidin form II.

N	Symop	R [Å]	Electron Density	E_ele	E_pol	E_dis	E_rep	E_tot
1	-x, -y, -z	10.01	B3LYP/6-31G(d,p)	-18.4	-7.0	-20.6	18.4	-31.2
1	-x, -y, -z	5.76	B3LYP/6-31G(d,p)	-4.7	-3.7	-35.7	18.1	-27.6
2	-x, y+1/2, -z+1/2	9.31	B3LYP/6-31G(d,p)	-7.5	-3.0	-9.4	5.9	-14.7
2	-x, y+1/2, -z+1/2	7.91	B3LYP/6-31G(d,p)	-15.4	-6.0	-23.2	30.2	-22.2
1	-x, -y, -z	9.20	B3LYP/6-31G(d,p)	-20.6	-2.5	-38.2	28.3	-39.4
2	x, -y+1/2, z+1/2	4.83	B3LYP/6-31G(d,p)	-11.8	-6.0	-38.3	17.6	-39.4
1	-x, -y, -z	12.41	B3LYP/6-31G(d,p)	-30.2	-4.6	-9.3	10.2	-37.2
2	x, y, z	12.47	B3LYP/6-31G(d,p)	-13.4	-2.3	-12.8	8.5	-21.8
1	x, -y+1/2, z+1/2	14.89	B3LYP/6-31G(d,p)	-7.0	-2.7	-5.8	6.0	-10.7

Table S6. Scale factors for benchmarked energy models (see: Mackenzie, C. F., Spackman, P. R., Jayatilaka, D. & Spackman, M. A. (2017). IUCrJ 4, 575-587).

Energy Model	k_ele	k_pol	k_disp	k_rep
CE-HF ... HF/3-21G electron densities	1.019	0.651	0.901	0.811
CE-B3LYP ... B3LYP/6-31G(d,p) electron densities	1.057	0.740	0.871	0.618

Table S7. Energy frameworks of total energy (blue) along with decomposed electrostatic (red) and dispersive (green) components for the crystal structures of furazidin. Energies with a magnitude less than 20 kJ mol^{-1} have been omitted.



The R², RMS, slope and intercept values of all model crystal structures re-optimized at DFT-D2 level of theory for forms I and II of furazidin

Table S8. DFT-D2 relative energy and linear regression data obtained after comparison of the calculated and experimental ¹H and ¹³C NMR data for furazidin form II.

rank	relative energy (kJ/mol)	¹ H NMR data				¹³ C NMR data			
		R ²	intercept	slope	RMS (ppm)	R ²	intercept	slope	RMS (ppm)
1	0.00	0.7228	-1.594	33.75	0.84	0.9854	-1.008	169.41	3.92
2	0.03	0.6813	-1.323	31.82	0.93	0.9879	-1.019	170.68	3.57
3	1.73	0.9551	-1.085	30.83	0.30	0.9938	-1.002	169.34	2.55
4	6.34	0.8129	-1.107	30.75	0.65	0.9702	-1.006	170.68	5.65
5	6.65	0.7612	-1.137	31.12	0.76	0.9809	-0.981	165.65	4.50
6	14.13	0.8380	-1.119	30.55	0.60	0.9763	-1.009	171.01	5.03
7	15.94	0.8203	-1.017	30.25	0.64	0.9729	-1.013	172.31	5.38
8	18.17	0.7110	-1.464	32.41	0.87	0.9742	-1.023	172.62	5.25
9	18.21	0.8777	-1.174	31.01	0.51	0.9854	-0.988	167.04	3.93
10	18.61	0.9081	-1.014	30.34	0.43	0.9697	-1.000	171.34	5.70
11	19.65	0.7365	-1.505	33.58	0.82	0.9834	-1.008	170.76	4.20
12	22.22	0.9025	-1.195	31.37	0.45	0.9600	-0.997	169.72	6.58
13	25.10	0.6617	-1.448	32.98	0.97	0.9740	-0.993	169.79	5.27
14	30.08	0.7716	-1.610	33.77	0.74	0.9709	-1.019	173.18	5.59
15	31.81	0.6798	-0.779	28.87	0.94	0.9912	-1.010	170.22	3.03
16	33.80	0.9240	-1.199	31.61	0.39	0.9680	-1.001	171.23	5.86

Table S9. DFT-D2 relative energy and linear regression data obtained after comparison of the calculated and experimental (variant II) ^1H and ^{13}C NMR data for furazidin form I.

rank	relative energy (kJ/mol)	^1H NMR data				^{13}C NMR data			
		R ²	intercept	slope	RMS (ppm)	R ²	intercept	slope	RMS (ppm)
1	0.00	0.9633	-1.173	31.13	0.41	0.9944	-1.019	171.30	2.45
2	2.76	0.9249	-1.082	30.46	0.59	0.9892	-1.021	171.43	3.41
3	5.65	0.9452	-1.02	30.14	0.50	0.9943	-1.016	171.22	2.46
4	10.02	0.824	-0.974	29.65	0.96	0.9917	-0.981	164.90	2.99
5	10.55	0.9297	-1.059	30.41	0.57	0.9806	-1.017	171.96	4.58
6	10.91	0.802	-0.972	29.85	1.03	0.9820	-0.977	166.09	4.41
7	11.55	0.8651	-0.746	28.46	0.82	0.9756	-0.998	170.28	5.15
8	12.24	0.9451	-1.152	31.19	0.50	0.9856	-1.010	171.57	3.95
9	13.18	0.8971	-1.054	30.21	0.70	0.9820	-0.978	166.03	4.42
10	13.42	0.8025	-0.788	29.18	1.03	0.9916	-0.985	166.41	3.00
11	13.46	0.7995	-0.932	29.85	1.04	0.9783	-0.980	165.85	4.86
12	14.07	0.8653	-0.851	29.29	0.82	0.9875	-0.989	166.69	3.67
13	14.34	0.8754	-0.978	30.31	0.79	0.9835	-0.952	163.07	4.22
14	14.68	0.9278	-0.972	29.90	0.58	0.9677	-0.998	170.67	5.96
15	15.06	0.8708	-1.133	30.80	0.80	0.9859	-0.990	167.60	3.90
16	16.18	0.7923	-0.897	29.37	1.07	0.9874	-0.992	167.14	3.68
17	16.61	0.7758	-0.685	28.05	1.12	0.9873	-0.999	170.42	3.70
18	17.87	0.7822	-1.101	30.87	1.10	0.9887	-0.972	165.26	3.49
19	18.07	0.8524	-0.959	30.15	0.87	0.9826	-0.998	169.74	4.34
20	18.39	0.8202	-0.791	28.96	0.97	0.9750	-0.985	168.10	5.22
21	18.70	0.8668	-1.031	30.22	0.82	0.9850	-0.996	169.65	4.03
22	19.92	0.8468	-1.057	30.43	0.89	0.9887	-0.997	167.76	3.48
23	19.99	0.8934	-0.949	30.09	0.72	0.9743	-0.975	166.87	5.30
24	20.00	0.8305	-0.951	29.86	0.94	0.9800	-0.986	167.41	4.66
25	20.17	0.8042	-0.912	29.51	1.03	0.9910	-1.004	169.19	3.11
26	20.23	0.8389	-1.006	30.08	0.91	0.9787	-0.984	167.39	4.81
27	20.27	0.7680	-1.151	30.90	1.14	0.9913	-0.965	162.66	3.05
28	20.80	0.7908	-0.958	29.83	1.07	0.9880	-0.975	163.73	3.59
29	21.07	0.8988	-1.014	30.10	0.70	0.9883	-0.996	168.88	3.55

30	21.39	0.6847	-0.788	28.29	1.41	0.9814	-0.962	162.78	4.49
31	21.63	0.8070	-1.063	30.24	1.02	0.9949	-0.954	162.02	2.32
32	21.95	0.7480	-0.915	29.31	1.21	0.9851	-0.973	164.94	4.01
33	22.08	0.7279	-0.833	29.27	1.27	0.9818	-0.972	165.56	4.44
34	22.84	0.7638	-0.919	29.59	1.16	0.9896	-0.945	160.20	3.34
35	24.70	0.8577	-0.813	29.41	0.85	0.9861	-0.975	166.78	3.88
36	24.82	0.8410	-1.081	30.45	0.91	0.9799	-0.988	167.84	4.67
37	24.91	0.7467	-0.975	30.00	1.21	0.9833	-0.968	164.71	4.25
38	25.02	0.8233	-1.083	30.92	0.96	0.9835	-0.994	169.05	4.22
39	25.08	0.6689	-0.836	29.38	1.46	0.9788	-0.934	160.30	4.80
40	27.74	0.7732	-0.846	28.95	1.13	0.9835	-0.967	164.66	4.22
41	28.91	0.7546	-1.173	30.97	1.19	0.9811	-0.971	163.92	4.52
42	29.66	0.7329	-1.169	31.36	1.26	0.9868	-0.958	162.99	3.78

Table S10. DFT-D2 relative energy and linear regression data obtained after comparison of the calculated and experimental (variant II) ¹H and ¹³C NMR data for furazidin form I. These data are for structures obtained from an additional CSP search for the best conformer indicated by the data from Table S4 tested in the space groups given in this table.

space group	relative energy (kJ/mol)	¹ H NMR data			¹³ C NMR data			RMS (ppm)	
		R ²	intercept	slope	RMS	R ²	intercept		
)									
14	17.67	0.9195	-0.866	29.42	0.62	0.9909	-1.018	172.69	3.12
15	5.42	0.9400	-1.119	30.64	0.53	0.9860	-1.019	171.27	3.89
19	5.14	0.8963	-1.106	30.30	0.71	0.9860	-1.007	169.10	3.88
33	16.92	0.9049	-0.858	29.15	0.67	0.9902	-1.013	171.54	3.25
5	7.70	0.9225	-1.059	29.90	0.60	0.9916	-1.033	172.81	3.00
9	11.23	0.9030	-1.102	30.86	0.68	0.9914	-1.028	172.84	3.03